Well-Controlled Ring-Opening Polymerization of Cyclic Esters Catalyzed by Aluminum Amido Complexes: Kinetics and Mechanism

Junpeng Liu, Haiyan Ma

Shanghai Key Laboratory of Functional Materials Chemistry and Laboratory of Organometallic Chemistry, East China University of Science and Technology, 130 Meilong Road, Shanghai 200237, People's Republic of China
Correspondence to: H. Ma (E-mail: haiyanma@ecust.edu.cn)

Received 2 June 2014; accepted 4 August 2014; published online 00 Month 2014
DOI: 10.1002/pola.27359

ABSTRACT: A series of aluminum dimethyl complexes **1**–**6** bearing N-[2-(pyrrolidinyl)benzyl]anilido ligands were synthesized and well characterized. The molecular structure of complex **1** determined by an X-ray diffraction study indicates the bidentate chelating mode of the pyrrolidinyl-anilido ligand. In the absence of a coinitiator, these complexes exhibited excellent control toward the polymerizations of ε-caprolactone and *rac*-lactide, affording polyesters with quite narrow molecular weight distributions ($M_w/M_n = 1.04$–1.26). The end group analysis of ε−CL oligomer via ^{1}H NMR and ESI-TOF MS methods gave strong support to the hypothesis that the polymerization catalyzed by these aluminum complexes proceeds via a coordination-insertion mechanism involving a unique Al—N (amido) bond initiation. Via ^{1}H NMR scale oligomerization studies, it is suggested that the insertion of the first lactide monomer into Al—N bond of the complex is much easier than the insertion of lactide monomer into the newly formed Al—O (lactate) bond and might also be easier than the insertion of the first ε−CL monomer into Al—N bond. © 2014 Wiley Periodicals, Inc. J. Polym. Sci., Part A: Polym. Chem. **2014**, *00*, 000–000

KEYWORDS: aluminum complex; amido ligand; catalysis; polyesters; ring-opening polymerization

INTRODUCTION Structurally well-defined organometallic complexes demonstrate prominent superiority in catalyzing the ring-opening polymerization (ROP) of cyclic esters.[1,2] Among them, aluminum complexes have attracted significant research focus, especially in the field of isoselective ROP of *rac*-lactide (*rac*-LA).[3–17] Although a variety of aluminum complexes have been explored up to date, in principal, only those having at least one alkoxy ligand could initiate the polymerization of cyclic esters in a well-controlled manner.[1–7] Due to the difficulties encountered in synthesis and/or purification, structurally well-defined aluminum alkoxide complexes are still limited. To overcome this problem, many studies have involved the use of coinitiators, such as alcohols, to convert the easily prepared aluminum alkyl complexes to the corresponding aluminum alkoxide complexes *in situ*.[18–27] Nevertheless, the addition of such coinitiators often induced unpredictable reactions, for example, the dissociation of ancillary ligand from the metal center,[19] especially for aluminum complexes bearing multidentate ligands with only *N*-donors.[12,20–23]

Previously, we reported series of aluminum alkyl complexes bearing β-diketiminate and amidinate ligands.[13,28,29] All of them demonstrated sufficient catalytic activities toward the ROP of ε-caprolactone (ε−CL), and the amidinate aluminum methyl complexes were also moderately active for *rac*-LA polymerization.[28,29] However, for both systems, the polymerizations were poorly controlled, producing polymers with significantly deviated molecular weights and rather broad molecular weight distributions ($M_w/M_n = 1.66$–3.74). Further studies indicated that both Al—N and Al—CH_3 bonds in the amidinate aluminum methyl complexes participated in the initiation. The strategy of generating *in situ* the desired aluminum alkoxide species capable of executing control on the polymerization proved to be unsuccessful. The β-diketiminate aluminum ethyl complexes were unreactive toward isopropanol or benzyl alcohol even under violent reaction conditions, whereas the treatment of the amindinate aluminum complexes with isopropanol led to the release of free amindines. Similar results were also reported by Peng's group:[22] for aluminum complexes bearing N-alkyl substituted β-diketiminate ligands, the addition of benzyl alcohol led to the dissociation of the ligand from metal center. Therefore, aluminum complexes bearing multidentate ligands with only N-donors, which are also capable of initiating the ROP of cyclic esters in a well-controlled manner, are still less explored.

Very recently, we reported a series of aluminum alkyl complexes bearing bidentate N-[2-(1-piperidinyl)benzyl]anilino

Additional Supporting Information may be found in the online version of this article.

or N-(2-morpholinobenzyl)anilino ligands.[30] All complexes proved to be capable of initiating the ROP of *rac*-lactide with living features, providing narrowly distributed PLAs in the absence of a coinitiator. To further expand the ligand system, in this work several N-[2-(1-pyrrolidinyl)benzyl]anilines were synthesized. The corresponding aluminum dimethyl complexes were obtained and evaluated for the ROP of cyclic esters. Detailed kinetic and mechanistic studies were also performed to have a thorough understanding on these systems.

EXPERIMENTAL

Materials and Methods

All manipulations were carried out under a dry argon atmosphere using standard Schlenk techniques or an MBraun glove-box. Toluene and *n*-hexane were refluxed over sodium/benzophenone prior to use. Dichloromethane and chloroform-*d* were dried over calcium hydride. Benzene-d_6 was refluxed over sodium and distilled under argon. $AlMe_3$ (2.0 M solution in toluene, Aldrich) was used as received. 2-(1-Pyrrolidinyl)benzaldehyde was prepared according to the published procedure.[31] ε−CL (99%, Aldrich) was dried over CaH_2 for 24 h at 80 °C, then vacuum distilled and stored under argon. *rac*-Lactide and *L*-lactide (Aldrich) were recrystallized with dry toluene and then sublimated twice under vacuum at 80 °C. All other chemicals were commercially available and used after appropriate purification. Glassware and vials used in the polymerization were dried in an oven at 120 °C overnight and exposed to vacuum-argon cycle three times.

NMR spectra were recorded on a Bruker AVANCE-400 spectrometer with $CDCl_3$ or C_6D_6 as solvent (^{1}H: 400 MHz; ^{13}C: 100 MHz). Chemical shifts for ^{1}H and ^{13}C NMR spectra were referenced internally using the residual solvent resonances and reported relative to tetramethylsilane. Elemental analyses were performed on an EA-1106 instrument. Gel permeation chromatography (GPC) analyses were carried out on a Waters instrument (M515 pump, Optilab Rex injector) in THF at 40 °C, at a flow rate of 1 mL·min^{-1}, with narrowly distributed linear polystyrene samples ($10^3 < M_n < 2 \times 10^6$ g mol^{-1}) as calibration standards.

Syntheses of Aluminum Dimethyl Complexes

Synthesis of N-[2-(1-Pyrrolidinyl)benzyl]anilido aluminum dimethyl (1)

To a solution of 2-(1-pyrrolidinyl) benzaldehyde (3.50 g, 20.0 mmol) in benzene (80 mL), freshly distilled aniline (1.86 g, 20.0 mmol) and *para*-toluenesulfonic acid monohydrate (2 mg) were added at r.t. The reaction solution was refluxed for 12 h and the water formed in the reaction was separated by water segregator. The solution was then cooled and filtered. The filtrate was concentrated to dryness under vacuum and the crude product was dissolved in absolute alcohol (200 mL), followed by an addition of sodium borohydride (11.4 g, 0.3 mol). The mixture was heated to reflux for 36 h, and water was added, followed by extracting the solution with dichloromethane (15 mL × 3). The combined organic layer was dried over anhydrous $MgSO_4$. Evaporation of all the volatile under reduced pressure yielded the crude compound, which was further purified by column chromatograph eluted by anhydrous EtOH to provide yellow oil, characterized as N-[2-(1-pyrrolidinyl)benzyl]aniline (1.79 g, 95% purity, which could not be further purified). ^{1}H NMR (400 MHz, $CDCl_3$, δ): 7.35 (m, 1H, Ar—H), 7.23 (m, 3H, Ar—H), 7.01 (m, 1H, Ar—H), 6.90 (m, 1H, Ar—H), 6.75 (m, 1H, Ar—H), 6.67 (m, 2H, Ar—H), 4.36 (s with shoulder, 3H, Ar—CH_2 and NH), 3.24 (br, 4H, —NCH_2), 1.95 (br, 4H, —CH_2—). ^{13}C NMR (100 MHz, $CDCl_3$, δ): 148.7 (Ar—C), 148.6 (Ar—C), 130.2 (Ar—C), 129.2 (Ar—C), 127.9 (Ar—C), 120.6 (Ar—C), 118.3 (Ar—C), 117.2 (Ar—C), 116.6 (Ar—C), 115.0 (Ar—C), 112.8 (Ar—C), 51.2 (Ar—CH_2), 46.7 (—NCH_2), 25.0 (—CH_2—).

In the glove-box, trimethylaluminum (2 mL, 4.00 mmol, 2 M solution in toluene) was slowly added to a solution of the above yellow oil (1.00 g) in hexane (15 mL), and then the solution was stirred for 24 h at r.t. A large amount of white solids precipitated. The reaction mixture was filtered, and the solid was recrystallized with a mixture of dichloromethane and hexane at −20 °C to afford complex **1** as colorless crystals (0.380 g, 30.8%). ^{1}H NMR (400 MHz, $CDCl_3$, δ): 7.35 (dd, J = 7.5, 1.5 Hz, 1H, Ar—H), 7.28 (td, J = 7.5, 1.5 Hz, 1H, Ar—H), 7.22 (dd, J = 7.3, 1.1 Hz, 1H, Ar—H), 7.20–7.13 (m, 3H, Ar—H), 6.71 (d, J = 8.0 Hz, 2H, Ar—H), 6.58 (t, J = 8.0 Hz, 1H, Ar—H), 4.44 (s, 2H, Ar—CH_2), 3.51 (m, 4H, —NCH_2), 2.04 (m, 4H, —CH_2—), −0.89 (s, 6H, Al—CH_3). ^{13}C NMR (100 MHz, $CDCl_3$, δ): 154.2 (Ar—C), 144.9 (Ar—C), 134.6 (Ar—C), 132.1 (Ar—C), 128.8 (Ar—C), 127.9 (Ar—C), 127.1 (Ar—C), 119.0 (Ar—C), 114.5 (Ar—C), 114.4 (Ar—C), 54.1 (Ar—CH_2), 53.5 (NCH_2), 23.7 (CH_2), −10.4 (Al—CH_3). Calcd. for $C_{19}H_{25}AlN_2$: C, 74.00; H, 8.17; N, 9.08. Found: C, 73.80; H, 8.18; N, 9.08%.

Synthesis of 2-Methyl-N-[2-(1-pyrrolidinyl) benzyl]anilido aluminum dimethyl (2)

The procedure was similar to that of complex **1**. *o*-Toluidine (2.14 g, 20.0 mmol) was reacted with 2-(1-pyrrolidinyl)benzaldehyde (3.50 g, 20.0 mmol) and sequentially reduced with $NaBH_4$ (11.4 g, 0.30 mol). After work-up, light yellow oil was isolated, characterized mainly as 2-methyl-N-[2-(1-pyrrolidinyl)benzyl]aniline (1.73 g, 90% purity, which could not be further purified). ^{1}H NMR (400 MHz, $CDCl_3$, δ): 7.37 (dd, J = 7.6, 1.6 Hz, 1H, Ar—H), 7.27 (td, J = 7.6, 1.6 Hz, 1H, Ar—H), 7.18 (t, J = 7.8 Hz, 1H, Ar—H), 7.10 (d, J = 7.3 Hz, 1H, Ar—H), 7.06 (dd, J = 8.1, 1.0 Hz, 1H, Ar—H), 6.96 (td, J = 7.3, 1.0 Hz, 1H, Ar—H), 6.71 (m, 2H, Ar—H), 4.40 (br s, 3H, Ar—CH_2 and NH), 3.25 (m, 4H, —NCH_2), 2.18 (s, 3H, Ar—CH_3), 1.96 (m, 4H, —CH_2—). ^{13}C NMR (100 MHz, $CDCl_3$, δ): 148.9 (Ar—C), 146.6 (Ar—C), 130.6 (Ar—C), 130.0 (Ar—C), 129.2 (Ar—C), 128.1 (Ar—C), 127.3 (Ar—C), 122.1 (Ar—C), 120.8 (Ar—C), 116.9 (Ar—C), 116.7 (Ar—C), 109.8 (Ar—C), 51.1 (Ar—CH_2), 47.2 (—NCH_2), 25.1 (—CH_2—), 17.6 (Ar—CH_3).

The above light yellow oil (1.064 g) was treated with trimethylaluminum (2 mL, 4.00 mmol, 2 M solution in toluene) to

afford the target product as colorless crystals (0.399 g, 31.0%). ^{1}H NMR (400 MHz, $CDCl_3$, δ): 7.27 (d, $J = 7.2$ Hz, 1H, Ar—H), 7.21 (t, $J = 7.1$ Hz, 1H, Ar—H), 7.14 (t, $J = 7.1$ Hz, 1H, Ar—H), 7.11–7.05 (m, 2H, Ar—H), 6.99 (d, $J = 7.1$ Hz, 1H, Ar—H), 6.83 (d, $J = 8.0$ Hz, 1H, Ar—H), 6.56 (t, $J = 7.2$ Hz, 1H, Ar—H), 4.45 (s, 2H, Ar—CH_2), 3.46 (m, 4H, —NCH_2—), 2.26 (s, 3H, Ar—CH_3), 1.96 (m, 4H, —CH_2—), −1.10 (s, 6H, Al—CH_3). ^{13}C NMR (100 MHz, $CDCl_3$, δ): 153.8 (Ar—C), 144.7 Ar—C), 134.2 (Ar—C), 130.9 (Ar—C), 129.6 (Ar—C), 126.9 (Ar—C), 126.7 (Ar—C), 126.0 (Ar—C), 125.5 (Ar—C), 117.7 (Ar—C), 115.4(Ar—C), 114.7 (Ar—C), 54.4 (Ar—CH_2), 53.2 (NCH_2), 24.0 (CH_2), 19.8 (Ar—CH_3), −10.8 (Al—CH_3). Calcd. for $C_{20}H_{27}AlN_2$: C, 74.50; H, 8.44; N, 8.69. Found: C, 74.24; H, 8.46; N, 8.53%.

Synthesis of 4-Isopropyl-N-[2-(1-pyrrolidinyl) benzy]anilido aluminum dimethyl (3)

The procedure was similar to that of complex **1**. 4-Isopropsylaniline (2.70 g, 20.0 mmol) was reacted with 2-(1-pyrrolidinyl)benzaldehyde (3.50 g, 20.0 mmol) and sequentially reduced with $NaBH_4$ (11.4 g, 0.30 mol). After work-up, light yellow oil was isolated, characterized mainly as 4-isopropyl-N-[2-(1-pyrrolidinyl) benzyl]aniline (1.79 g, 90% purity, which could not be further purified). ^{1}H NMR (400 MHz, $CDCl_3$, δ): 7.31 (dd, $J = 7.5$, 1.5 Hz, 1H, Ar—H), 7.20 (td, $J = 8.0$, 1.5 Hz, 1H, Ar—H), 7.05 (d, $J = 8.4$ Hz, 2H, Ar—H), 6.96 (d, $J = 8.0$ Hz, 1H, Ar—H), 6.89 (td, $J = 7.5$, 0.75 Hz, 1H, Ar—H), 6.60 (d, $J = 8.4$ Hz, 2H, Ar—H), 4.30 (s, 2H, Ar—CH_2), 4.22 (br s, 1H, NH), 3.21 (m, 4H, —NCH_2), 2.81 (sept, $J = 6.8$ Hz, 1H, —$CH(CH_3)_2$), 1.92 (m, 4H, —CH_2—), 1.21 (d, $J = 6.8$ Hz, 6H, —$CH(CH_3)_2$). ^{13}C NMR (100 MHz, $CDCl_3$, δ): 148.4 (Ar—C), 146.4 (Ar—C), 137.3 (Ar—C), 130.1 (Ar—C), 129.0 (Ar—C), 127.6 (Ar—C), 126.8 (Ar—C), 120.3 (Ar—C), 116.2 (Ar—C), 112.5 (Ar—C), 50.9 (Ar—CH_2), 46.7 (NCH_2), 32.9 [$CH(CH_3)_2$], 24.7 (CH_2), 24.1 [$CH(CH_3)_2$].

The above light yellow oil (1.18 g) was treated with trimethylaluminum (2 mL, 4.00 mmol, 2 M solution in toluene) to afford the target product as colorless crystals (0.468 g, 33.4%). ^{1}H NMR (400 MHz, $CDCl_3$, δ): 7.33 (dd, $J = 7.4$, 1.7 Hz, 1H, Ar—H), 7.27 (td, $J = 7.9$, 1.7 Hz, 1H, Ar—H), 7.21 (td, $J = 7.4$, 1.0 Hz, 1H, Ar—H), 7.15 (d, $J = 7.9$, 1.0 Hz, 1H, Ar—H), 7.05 (d, $J = 8.0$ Hz, 2H, Ar—H), 6.66 (d, $J = 8.0$ Hz, 2H, Ar—H), 4.44 (s, 2H, Ar—CH_2), 3.51 (m, 4H, —NCH_2), 2.80 (sept, $J = 6.9$ Hz, 1H, $CH(CH_3)_2$), 2.04 (m, 4H, —CH_2—), 1.21 (d, $J = 6.9$ Hz, 6H, $CH(CH_3)_2$), −0.93 (s, 6H, Al—CH_3). ^{13}C NMR (100 MHz, $CDCl_3$, δ): 152.2 (Ar—C), 144.9 (Ar—C), 134.74 (Ar—C), 134.70 (Ar—C), 132.0 (Ar—C), 127.8 (Ar—C), 127.0 (Ar—C), 126.7 (Ar—C), 119.0 (Ar—C), 114.0 (Ar—C), 54.0 (Ar—CH_2), 53.8 (NCH_2), 33.0 [$CH(CH_3)_2$], 24.3 (CH_2), 23.7 [$CH(CH_3)_2$], −10.3 (Al—CH_3). Calcd. for $C_{22}H_{31}AlN_2$: C, 75.39; H, 8.92; N, 7.99. Found: C, 74.92; H, 8.95; N, 8.13%.

Synthesis of 2-Chloro-N-[2-(1-pyrrolidinyl) benzyl]anilido aluminum dimethyl (4)

The procedure was similar to that of complex **1**. 2-Chloroaniline (2.54 g, 20.0 mmol) was reacted with 2-(1-pyrrolidinyl)benzaldehyde (3.50 g, 20.0 mmol) and sequentially reduced with $NaBH_4$ (11.4 g, 0.30 mol). After work-up, light yellow solids were isolated mainly as 2-chloro-N-[2-(1-pyrrolidinyl)benzyl]aniline (1.92 g, 95% purity, which could not be further purified). ^{1}H NMR (400 MHz, $CDCl_3$, δ): 7.27 (d, $J = 7.5$ Hz, 1H, Ar—H), 7.21 (dd, $J = 8.0$, 1.3 Hz, 1H, Ar—H), 7.18 (td, $J = 7.4$, 1.3 Hz, 1H, Ar—H), 7.08 (td, $J = 7.8$, 1.3 Hz, 1H, Ar—H), 6.98 (d, $J = 8.0$ Hz, 1H, Ar—H), 6.88 (t, $J = 7.3$ Hz, 1H, Ar—H), 6.62 (d, $J = 8.0$ Hz, 1H, Ar—H), 6.58 (td, $J = 7.5$, 1.0 Hz, 1H, Ar—H), 4.33 (s, 2H, phenyl—CH_2), 3.14 (m, 4H, —NCH_2), 1.89 (m, 4H, —CH_2—). ^{13}C NMR (100 MHz, $CDCl_3$, δ): 148.7 (Ar—C), 144.1 (Ar—C), 129.9 (Ar—C), 128.9 (Ar—C), 128.7 (Ar—C), 127.9 (Ar—C), 127.7 (Ar—C), 120.8 (Ar—C), 119.1 (Ar—C), 116.9 (Ar—C), 116.8 (Ar—C), 111.2 (Ar—C), 51.0 (Ar—CH_2), 46.4 (NCH_2), 24.9 (CH_2).

The solution of above light yellow solids (1.14 g) in hexane was treated with trimethylaluminum (2 mL, 4.00 mmol, 2 M solution in toluene) to afford the target product as colorless crystals (0.526 g, 38.5%). ^{1}H NMR (400 MHz, $CDCl_3$, δ): 7.35 (d, $J = 7.4$ Hz, 1H, Ar—H), 7.30 (td, $J = 7.8$, 1.5 Hz, 1H, Ar—H), 7.23 (m, 2H, Ar—H), 7.17 (m, 2H, Ar—H), 6.81 (d, $J = 8.1$ Hz, 1H, Ar—H), 6.67 (td, $J = 7.5$, 1.0 Hz, 1H, Ar—H), 4.44 (s, 2H, Ar—CH_2), 3.50 (br, 4H, —NCH_2), 2.02 (m, 4H, —CH_2—), −0.94 (s, 6H, Al—CH_3). ^{13}C NMR (100 MHz, $CDCl_3$, δ): 151.9 (Ar—C), 146.4 (Ar—C), 133.8 (Ar—C), 132.2 (Ar—C), 129.0 (Ar—C), 128.3 (Ar—C), 127.7 (Ar—C), 126.8 (Ar—C), 122.3 (Ar—C), 118.6 (Ar—C), 115.7 (Ar—C), 114.7 (Ar—C), 54.6 (Ar—CH_2), 54.1 (NCH_2), 24.3 (CH_2), −9.2 (Al—CH_3). Calcd. for $C_{19}H_{24}AlClN_2$: C, 66.56; H, 7.06; N, 8.17. Found: C, 66.48; H, 7.20; N, 7.85%.

Synthesis of 3-Chloro-N-[2-(1-pyrrolidinyl) benzyl]anilido aluminum dimethyl (5)

The procedure was similar to that of complex **1**. 3-Chloroaniline (2.54 g, 20.0 mmol) was reacted with 2-(1-pyrrolidinyl)benzaldehyde (3.50 g, 20.0 mmol) and sequentially reduced with $NaBH_4$ (11.4 g, 0.30 mol). After work-up, light yellow solids were isolated mainly as 3-chloro-N-[2-(1-pyrrolidinyl)benzyl]aniline (1.83 g, 80% purity, which could not be further purified). ^{1}H NMR (400 MHz, $CDCl_3$, δ): 7.25 (dd, $J = 7.5$, 1.5 Hz, 1H, Ar—H), 7.20 (td, $J = 7.4$, 1.5 Hz, 1H, Ar—H), 7.03 (t, $J = 8.0$ Hz, 1H, Ar—H), 6.96 (t, $J = 7.3$ Hz, 1H, Ar—H), 6.88 (td, $J = 7.5$, 1.0 Hz, 1H, Ar—H), 6.63 (d, $J = 8.0$ Hz, 1H, Ar—H), 6.59 (t, $J = 2.0$ Hz, 1H, Ar—H), 6.45 (dd, $J = 8.0$, 2.0 Hz, 1H, Ar—H), 4.45 (br, 1H, —NH), 4.26 (br s, 2H, Ar—CH_2), 3.16 (m, 4H, —NCH_2), 1.90 (m, 4H, —CH_2—). ^{13}C NMR (100 MHz, $CDCl_3$, δ): 149.5 (Ar—C), 148.6 (Ar—C), 134.9 (Ar—C), 130.12 (Ar—C), 130.16 (Ar—C), 128.4 (Ar—C), 128.0 (Ar—C), 120.6 (Ar—C), 116.9 (Ar—C), 116.7 (Ar—C), 112.2 (Ar—C), 111.0 (Ar—C), 51.1 (Ar—CH_2), 46.5 (—NCH_2), 24.9 (—CH_2—).

The solution of above light yellow solids (1.14 g) in hexane was treated with trimethylaluminum (2 mL, 4.00 mmol, 2 M solution in toluene) to afford the target product as colorless crystals (0.583 g, 42.6%). ^{1}H NMR (400 MHz, $CDCl_3$, δ): 7.34 (d, $J = 7.3$ Hz, 1H, Ar—H), 7.29 (td, $J = 7.9$, 1.7 Hz, 1H, Ar—H), 7.23 (td, $J = 7.3$, 1.0 Hz, 1H, Ar—H), 7.17 (d, $J = 7.9$

Hz, 1H, Ar—H), 7.02 (t, $J = 7.9$ Hz, 1H, Ar—H), 6.64 (t, $J = 1.9$ Hz, 1H, Ar—H), 6.58 (dd, $J = 8.0$, 1.9 Hz, 1H, Ar—H), 6.54 (dd, $J = 8.0$, 1.9 Hz, 1H, Ar—H), 4.38 (s, 2H, Ar—CH_2), 3.50 (m, 4H, —NCH_2), 2.05 (br, 4H, —CH_2—), −0.90 (s, 6H, Al—CH_3). ^{13}C NMR (100 MHz, $CDCl_3$, δ): 155.6 (Ar—C), 144.8 (Ar—C), 134.7 (Ar—C), 134.0 (Ar—C), 132.1 (Ar—C), 129.3 (Ar—C), 128.2 (Ar—C), 127.3 (Ar—C), 119.0 (Ar—C), 114.3 (Ar—C), 113.9 (Ar—C), 113.1 (Ar—C), 54.2 (Ar—CH_2), 53.4 (NCH_2), 23.8 (CH_2), −10.5 (Al—CH_3). Calcd. for $C_{19}H_{24}AlClN_2$: C, 66.56; H, 7.06; N, 8.17. Found: C, 65.97; H, 7.04; N, 8.07%.

Synthesis of 4-Chloro-N-[2-(1-pyrrolidinyl) benzy]anilido aluminum dimethyl (6)

The procedure was similar to that of complex **1**. 4-Chloroaniline (2.54 g, 20.0 mmol) was reacted with 2-(1-pyrrolidinyl)benzaldehyde (3.50 g, 20.0 mmol) and sequentially reduced with $NaBH_4$ (11.4 g, 0.30 mol). After work-up, colorless solids were isolated, characterized mainly as 4-chloro-N-[2-(1-pyrrolidinyl)benzyl] aniline (1.97 g, 90% purity, which could not be further purified). ^{1}H NMR (400 MHz, $CDCl_3$, δ): 7.27 (dd, $J = 7.3$, 1.3 Hz, 1H, Ar—H), 7.18 (td, $J = 7.6$, 1.3 Hz, 1H, Ar—H), 7.10 (m, 2H, Ar—H), 6.97 (d, $J = 8.8$ Hz, 2H, Ar—H), 6.54 (d, $J = 8.8$ Hz, 2H, Ar—H), 4.39 (br, 1H, NH), 4.27 (s, 2H, Ar—CH_2), 3.17 (m, 4H, —NCH_2), 1.91 (m, 4H, —CH_2—). ^{13}C NMR (100 MHz, $CDCl_3$, δ): 148.9 (Ar—C), 147.2 (Ar—C), 130.3 (Ar—C), 129.2 (Ar—C), 128.9 (Ar—C), 128.3 (Ar—C), 122.0 (Ar—C), 120.9 (Ar—C), 117.0 (Ar—C), 114.0 (Ar—C), 51.4 (Ar—CH_2), 47.1 (NCH_2), 25.2 (CH_2).

The solution of above solids (1.14 g) in hexane was treated with trimethylaluminum (2 mL, 4.00 mmol, 2 M solution in toluene) to afford the target product as colorless crystals (0.564 g, 41.0%). ^{1}H NMR (400 MHz, $CDCl_3$, δ): 7.35 (dd, $J = 7.2$, 1.2 Hz, 1H, Ar—H), 7.29 (td, $J = 7.8$, 1.6 Hz, 1H, Ar—H), 7.22 (td, $J = 7.8$, 1.2 Hz, 1H, Ar—H), 7.17 (dd, $J = 7.2$, 1.6 Hz, 1H, Ar—H), 7.08 (d, $J = 8.9$ Hz, 2H, Ar—H), 6.60 (d, $J = 8.9$ Hz, 2H, Ar—H), 4.38 (s, 2H, Ar—CH_2), 3.50 (m, 4H, —NCH_2), 2.04 (m, 4H, —CH_2—), −0.91 (s, 6H, Al—CH_3). ^{13}C NMR (100 MHz, $CDCl_3$, δ): 152.8 (Ar—C), 144.8 (Ar—C), 134.2 (Ar—C), 132.2 (Ar—C), 128.5 (Ar—C), 128.1 (Ar—C), 127.2 (Ar—C), 119.05 (Ar—C), 119.00 (Ar—C), 115.3 (Ar—C), 54.2 (Ar—CH_2), 53.6 (NCH_2), 23.7 (CH_2), −10.5 (Al—CH_3). Calcd. for $C_{19}H_{24}AlClN_2$: C, 66.56; H, 7.06; N, 8.17 %. Found: C, 66.83; H, 6.99; N, 8.22%.

X-Ray Crystallography

Single crystals of complex **1** suitable for X-ray diffraction studies were obtained from a saturated hexane-dichloromethane solution at −20 °C. The crystallographic data for complex **1** was collected on a Bruker SMART APEX diffractometer with graphite-monochromated Mo-Kα radiation ($\lambda = 0.71073$ Å). All data were collected at −20 °C using omega-scan techniques. The structure of complex **1** was solved by direct methods and subsequently refined on F^2 by full-matrix least-squares methods using the SHELXTL program package.[32] SADABS absorption corrections were applied to the data. All non-hydrogen atoms were refined anisotropically.[33] Hydrogen atoms of **1** were treated using a riding model and refined by the geometry method. Molecule structure was generated using ORTEP III program.[34]

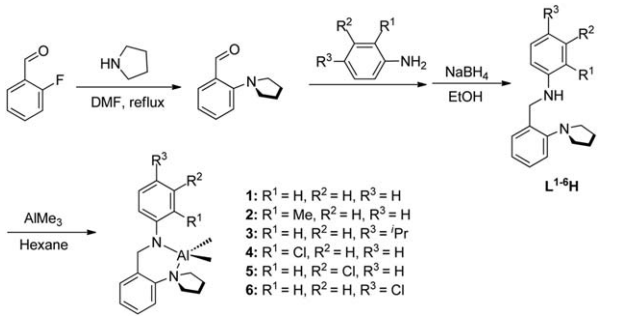

SCHEME 1 Synthesis of aluminum dimethyl complexes **1–6**.

Polymerization Procedure

In a glove-box, a proper amount of ε−CL (in toluene) or *rac*-LA was added to a Schlenk tube, and a certain amount of toluene and the solution of aluminum complex in toluene were injected sequentially ([ε−CL] = 4 mol/L, [ε-CL]$_0$/[Al]$_0$ = 100; or [*rac*-LA] = 1 mol/L, [*rac*-LA]$_0$/[Al]$_0$ = 100). The tube was taken out of the glove-box and immerged into an oil bath stabilized at desired temperature. The mixture was stirred for a specific time interval and then quenched with wet petroleum ether. Monomer conversion was monitored by integration of monomer vs. polymer methine (for *rac*-lactide) or methylene (for ε−CL) resonance in the ^{1}H NMR spectrum ($CDCl_3$, 400 MHz) after removal of the volatiles. The purification of the polymer was managed by dissolving the crude sample in CH_2Cl_2 and precipitating the polymer solution with methanol. The obtained polymer was further dried in a vacuum oven at 60 °C for 36 h and subjected to GPC measurement.

RESULTS AND DISCUSSION

Synthesis and Characterization of Aluminum Dimethyl Complexes 1–6

As shown in Scheme 1, the nucleophilic substitution reaction between pyrrolidine and 2-fluorobenzaldehyde afforded 2-(1-pyrrolidinyl) benzaldehyde; then it was condensed with substituted anilines and sequentially reduced with sodium borohydride to produce the target N-[2-(1-pyrrolidinyl)benzyl]aniline proligands $\mathbf{L^{1-6}H}$. Due to the strong hygroscopicity of these compounds and their similar polarity to the starting anilines, all of them could not be isolated in an analytically pure form.

Unlike the previously reported N-[2-(1-piperidinyl)benzyl]aniline system,[30] the reaction of proligands $\mathbf{L^{1-6}H}$ with one equiv. of $AlMe_3$ at r.t. readily afforded the target aluminum dimethyl complexes **1–6** (Scheme 1). No production of the trimethylaluminum adduct with the neutral ligand was detected. In the ^{1}H NMR spectra of complexes **1–6**, the signal of Al-CH_3 is observed at $-0.89 \sim -1.10$ ppm as a characteristic singlet. The resonance of NCH_2 (pyrrolidinyl) at around 3.50 ppm is significantly downfield shifted in comparison with that of the

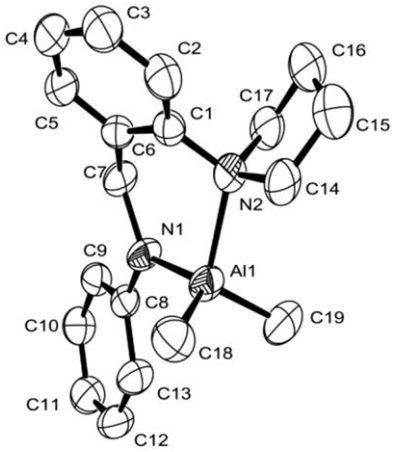

FIGURE 1 ORTEP drawing of **1** (thermal ellipsoids drawn at the 50% probability level). Selected bond lengths [Å] and angles [°]: Al1-N1 1.8583(17), Al1-N2 2.0130(19), Al1-C18 1.963(2), Al1-C19 1.968(3). N1-Al1-C18 114.74(10), N1-Al1-C19 113.43(10), C18-Al1-C19 118.61(11), N1-Al1-N2 96.62(7), C18-Al1-N2 103.87(9), C19-Al1-N2 105.99(10), C8-N1-C7 116.38(15), C8-N1-Al1 121.99(13), C7-N1-Al1 121.37(13), C1-N2-C17 109.13(15), C1-N2-C14 114.75(16), C17-N2-C14 102.42(17), C1-N2-Al1 110.20(13), C17-N2-Al1 115.61(14), C14-N2-Al1 104.66(13).

proligand (3.14–3.24 ppm), indicative of the coordination of pyrrolidinyl-N donor to aluminum center in these complexes.

The molecular structure of complex **1** with selected bond lengths and bond angles is shown in Figure 1. Complex **1** crystallizes in a monoclinic space group P2(1)/c, and the aluminum center is coordinated by the two nitrogen donors of the ligand and two methyl groups in a distorted tetrahedral geometry. The N1-Al1-N2 bond angle of 96.62(7)°, smaller than the ideal tetrahedral bond angle of 109.5°, is close to those in related known Al complexes.[11]

The Al1-N1 bond length of 1.8583(17) Å is significantly shorter than the Al1-N2 bond length of 2.0130(19) Å, implying the difference between the amido N1 atom and the amine N2 atom in bonding with the aluminum center. Interestingly, the nitrogen atom N1 is roughly in a planar fashion surrounded by C7, C8 and Al1 with the sum of the corresponding bond angles being 359.7°, which might imply some double bonding character of Al1-N1 bond. The N2 atom has a distorted tetrahedral environment in which the C17-N2-Al1 and C14-N2-Al1 have different bond angles of 115.61(14)° and 104.66(13)°, probably due to the steric requirements of the two methyl ligands.

Moreover, the alcoholysis reaction of complexes **1–6** failed to afford the desired N-[2-(1-pyrrolidinyl)benzyl]anilino aluminum alkoxide complexes. The reaction of representative complex **6** with isopropanol led to the production of the free ligand $\mathbf{L^6H}$ and some undissolvable solids (see Supporting Information), which hampered a further understanding on the reaction.

ROP of ε−CL

The ROP of ε−CL was studied at 35 and 45 °C in toluene by using aluminum complexes **1–6** as single component

TABLE 1 The ROP of ε−CL Initiated by Complexes **1–6**[a]

Run	Cat.	Temp. (°C)	Time (min)	Conv. (%)[b]	$M_{n,\ calcd}$[c] ($\times 10^4$)	$M_{n,\ NMR}$[d] ($\times 10^4$)	M_n'[e] ($\times 10^4$)	M_w/M_n[e]
1	**1** (H)	35	40	34	0.39	0.41	0.52	1.07
2		35	150	83	0.95	0.94	0.92	1.04
3		45	60	90	1.03	1.10	1.23	1.11
4	**2** (*o*-Me)	35	40	19	0.22	0.21		
5		35	210	84	0.96	0.98	0.82	1.15
6		45	90	83	0.95	1.01	0.73	1.06
7	**3** (*p*-^{i}Pr)	35	40	30	0.34	0.41	0.55	1.04
8		35	150	81	0.92	0.92		
9		45	60	88	1.00	1.11	1.09	1.09
10	**4** (*o*-Cl)	35	40	20	0.23	0.28		
11		35	210	87	0.99	1.10	0.90	1.11
12		45	90	86	0.98	1.13	1.05	1.14
13	**5** (*m*-Cl)	35	40	39	0.44	0.52	0.51	1.04
14		45	60	96	1.09	1.16	1.37	1.07
15	**6** (*p*-Cl)	35	40	35	0.34	0.41		
16		45	60	92	1.05	1.25	0.99	1.04

[a] $[\varepsilon\text{−CL}]_0 = 4.0$ M, $[\varepsilon\text{−CL}]_0/[\text{Al}]_0 = 100$, in toluene.
[b] Determined by the integration ratio of the methylene protons in monomer and polymer in $CDCl_3$.
[c] $M_{n,calcd} = ([\varepsilon\text{−CL}]_0/[\text{Al}]_0) \times 114.14 \times$ conv. (%). + mass of the free ligand.
[d] Determined by the integration ratio of the methylene protons in polymer main chain versus the characteristic resonance of the amido ligand.
[e] The number average molecular weight (M_n) and molecular weight distribution (M_w/M_n) were determined by a gel permeation chromatograph in THF at 40 °C, using narrowly distributed polystyrenes as standards, $M_n' = 0.56 \times M_n$.

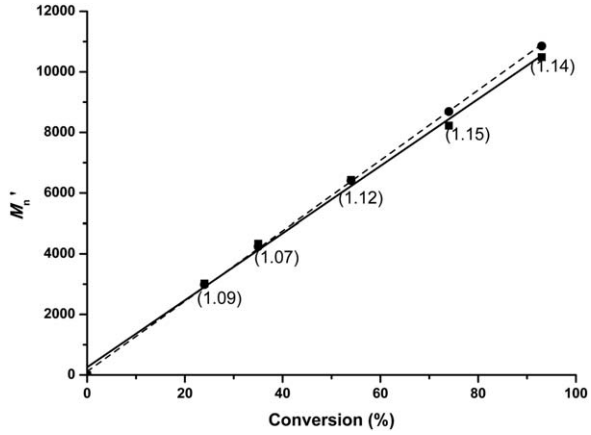

FIGURE 2 Plots of M_n' versus monomer conversion for ε−CL polymerization and PDI valves using complex **1** as initiator (in toluene, 35 °C, $[\varepsilon\text{−CL}]_0 = 4$ mol/L, $[\varepsilon\text{−CL}]_0/[\text{Al}]_0 = 100$. ■: GPC values; ●: Theoretic values).

initiators ($[\varepsilon\text{−CL}]_0$:$[\text{Al}]_0$hx2009;= 100:1), and the results are summarized in Table 1. All these aluminum complexes proved to be active initiators toward the polymerization of ε−CL, and high monomer conversions up to 96% could be reached within 1–4 h by adopting a monomer concentration of 4.0 mol/L. It is found that the nature and position of the substituent on the anilino moiety of the supporting ligand have different effects on the catalytic activity of these complexes. In all cases, the introduction of an *ortho*-substituent to the anilino moiety leads to an obvious decrease of the catalytic activity [**2** (*o*-Me) and **4** (*o*-Cl) vs. **1** (H)], implying that the steric hindrance around the metal center is unfavorable for the polymerization. In contrast to the dominant steric effect played by an *ortho*-chloro group in complex **4**, the electron-withdrawing effect of a chloro-group at the *meta*- or *para*-position of the anilino moiety seems to be more crucial. Both complexes **5** (*m*-Cl) and **6** (*p*-Cl) show higher catalytic activities than the rest aluminum complexes, and complex **5** is more active than complex **6**. The benefit of an electron-withdrawing group at these positions is also witnessed by the lower activity of complex **3** (*p*-^{i}Pr) in comparison with that of complex **1**. All these results are however similar to those reported previously for aluminum complexes with analogous piperidinyl-anilino ligands.[30]

As shown in Table 1, PCLs with very narrow molecular weight distributions ($M_w/M_n = 1.04$–1.15) are provided by these aluminum complexes. The corrected number average molecular weights (M_n') of the polymers ($M_n' = 0.56 \times M_n$; M_n, determined by GPC)[35] approximately match the theoretical values calculated on the assumption that each active metal center initiates one polymer chain. Furthermore, a linear relationship between M_n' and the conversion of ε−CL monomer could be observed over the entire conversion range with complex **1** as the initiator (Figure 2). All these features imply some living characters of the polymerization.

To have a better understanding on the polymerization process initiated by these aluminum complexes, the kinetics of

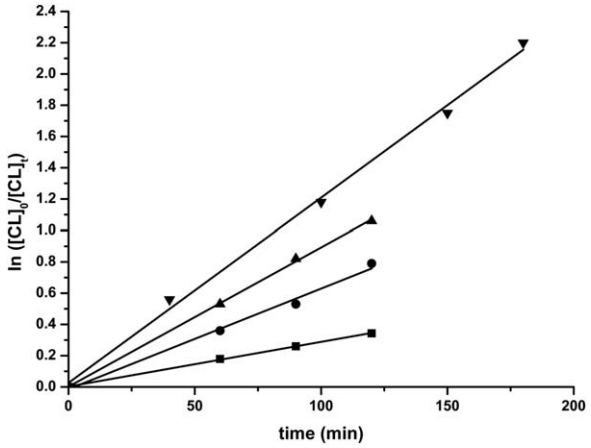

FIGURE 3 Plots of $\ln([\varepsilon\text{−CL}]_0/[\varepsilon\text{−CL}]_t)$ versus time for ε−CL polymerization using complex **1** as initiator (in toluene, 35 °C, $[\varepsilon\text{−CL}]_0 = 4$ mol/L. ■: $[\text{Al}]_0 = 0.01$ mol/L, $k_{app} = 4.85 \times 10^{-5} \pm 0.800 \times 10^{-6}$ s^{-1}; ●: $[\text{Al}]_0 = 0.02$ mol/L, $k_{app} = 9.73 \times 10^{-5} \pm 6.67 \times 10^{-6}$ s^{-1}; ▲: $[\text{Al}]_0 = 0.03$ mol/L, $k_{app} = 1.47 \times 10^{-4} \pm 2.67 \times 10^{-6}$ s^{-1}; ▼: $[\text{Al}]_0 = 0.04$ mol/L, $k_{app} = 1.97 \times 10^{-4} \pm 6.33 \times 10^{-6}$ s^{-1}).

ε−CL polymerization with complex **1** as the initiator was studied in detail. The semilogarithmic plots of $\ln([\varepsilon - \text{CL}]_0/[\varepsilon - \text{CL}]_t)$ versus reaction time (t) at different initiator concentrations are shown in Figure 3. The plots exhibit perfect linear relationship and no obvious induction period is observed in each case, indicating the first order dependence of the polymerization on monomer concentration. Thus, the polymerization of ε−CL by complex **1** proceeds according to eq 1, where $k_{app} = k_p[\text{Al}]^x$, k_{app} and k_p are the apparent propagation and propagation rate constants, respectively. The order in aluminum concentration (x) was determined by plotting $\ln k_{app}$ vs. $\ln[\text{Al}]_0$, and a straight line was obtained with a slope of 1.09 (Figure 4). So the polymerization of ε−CL follows an overall kinetic law given by eq 2 with $k_p = 0.052$ L·mol^{-1}·s^{-1}. That is, the rate determining step involves one metal center and one monomer molecule stoichiometrically.

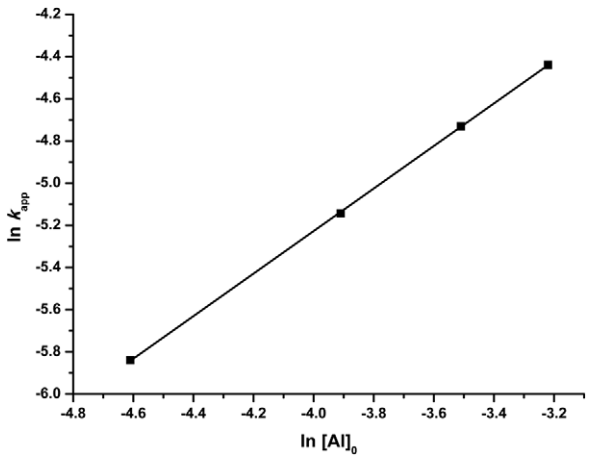

FIGURE 4 Plot of $\ln k_{app}$ versus $\ln[\text{Al}]_0$ for ε−CL polymerization using complex **1** as initiator (in toluene, 35 °C, $[\varepsilon\text{−CL}]_0 = 4$ mol/L; slope = 1.09).

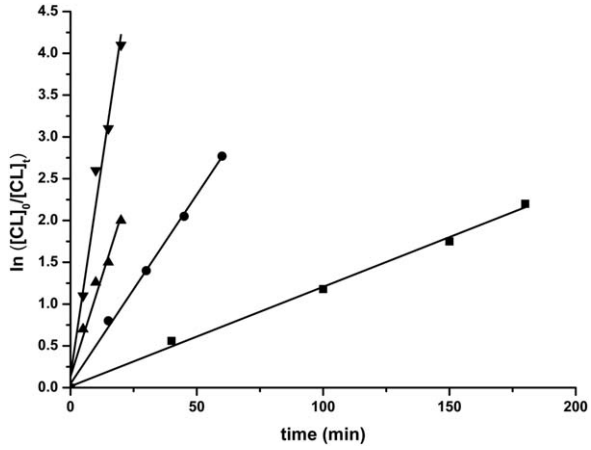

FIGURE 5 Plots of $\ln([\varepsilon-\mathrm{CL}]_0/[\varepsilon-\mathrm{CL}]_t)$ versus time for $\varepsilon-$CL polymerization using complex **1** as initiator at different temperatures (in toluene, $[\varepsilon-\mathrm{CL}]_0 = 4$ mol/L, $[\varepsilon-\mathrm{CL}]_0/[\mathrm{Al}]_0 = 100$. ■: T = 35 °C, $k_{app} = 1.97 \times 10^{-4} \pm 6.33 \times 10^{-6}$ s^{-1}; ●: T = 45 °C, $k_{app} = 0.755 \times 10^{-3} \pm 0.192 \times 10^{-4}$ s^{-1}; ▲: T = 55 °C, $k_{app} = 1.60 \times 10^{-3} \pm 1.50 \times 10^{-4}$ s^{-1}; ▼: T = 65 °C, $k_{app} = 3.40 \times 10^{-3} \pm 2.88 \times 10^{-4}$ s^{-1}).

$$-\mathrm{d}[\varepsilon-\mathrm{CL}]_t/\mathrm{d}t = k_{app}[\varepsilon-\mathrm{CL}]_t \quad (1)$$

$$-\mathrm{d}[\varepsilon-\mathrm{CL}]_t/\mathrm{d}t = k_p[\mathrm{Al}][\varepsilon-\mathrm{CL}]_t \quad (2)$$

Using complex **1** as the initiator, conversions of $\varepsilon-$CL in toluene at various temperatures of 35, 45, 55, and 65 °C with fixed monomer and initiator concentrations were monitored via ^{1}H NMR spectroscopy. By plotting $\ln([\varepsilon-\mathrm{CL}]_0/[\varepsilon-\mathrm{CL}]_t)$ versus time (t) (Figure 5), k_{app} values at different temperatures could be obtained and therefore the k_p values according to $k_{app} = k_p[\mathrm{Al}]_0$. Based on the Eyring equation, the thermodynamics curve of $\ln(k_p/T)$ vs. $1/T$ was plotted (Figure 6). From the slope and intercept of the curve, the transition enthalpy $\Delta H^{\neq} = 78.11 \pm 7.43$ KJ/mol and entropy $\Delta S^{\neq} = -25.57 \pm 2.53$ J/(mol·K) could be obtained, which then enabled the calculation of the transition activation Gibbs free energy, $\Delta G^{\neq} = \Delta H^{\neq} - T\Delta S^{\neq} = 85.72$ kJ/mol at 298 K. The positive enthalpy and negative entropy imply the endothermic nature of the polymerization.

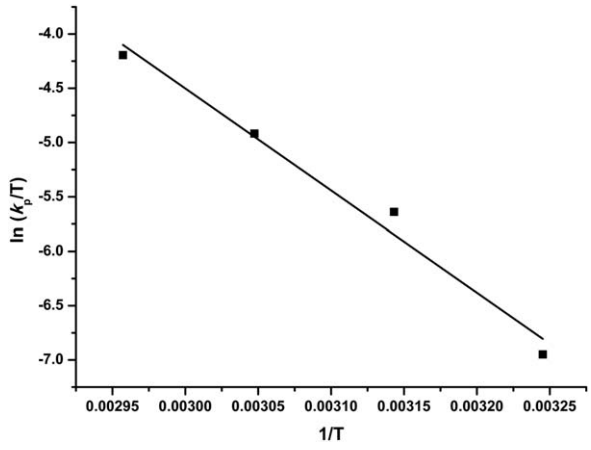

FIGURE 6 Plot of $\ln(k_p/T)$ versus $1/T$ for ε-CL polymerization using complex 1 as initiator.

To gain some insight into how these complexes, acting as single component catalysts, initiated the ROP of ε-CL and the role played by the bidentate pyrrolidinyl-anilido ligands during the polymerization, the NMR scale reaction of complex **6** with ε-CL ($[\mathrm{CL}]_0$:$[\mathbf{6}]_0 = 9$) in C_6D_6 was carried out (see Supporting Information). In the ^{1}H NMR spectrum measured at 15 °C, the resonances attributable to the pyrrolidinyl-anilido ligand as well as Al-CH_3 groups could still be identified unambiguously, which however are slightly different from those of complex **6**. For instance, one multiplet assignable to NCH_2 (pyrrolidinyl) is displayed at 2.84 ppm, instead of two multiple signals at 2.84 and 2.72 ppm for complex **6**. Besides, a tiny, broad signal at 5.11 ppm as well as one multiplet at 2.70 ppm in stoichiometric ratio could be observed. Upon slightly warming the reaction mixture at 25 °C for about 30 min, the signals at 5.11 and 2.70 ppm became apparent and the gradual oligomerization occurred. After standing at 45 °C overnight, the monomer was almost consumed and the species represented by the signals at 5.11 and 2.70 ppm became the only identifiable species. The signals of aluminum methyl groups at the high field region were still observable (see Supporting Information). Based on these features, we suggest that at a relatively low temperature the treatment of complex **6** with excess $\varepsilon-$CL leads to the formation of monomer-coordinated species, where the nitrogen atom of pyrrolidinyl may dissociate from the metal center. The minor species formed upon slightly warming is the monomer-inserted active species, which initiate the polymerization of $\varepsilon-$CL. The significant downfield shift of ArCH_2 proton signal from 4.15 ppm (complex **6**) to 5.11 ppm during this process is likely due to the insertion of the monomer into the Al-N (amido) bond (see Supporting Information).

End-group analysis of a typical ε-CL oligomer obtained by using complex **1** as the initiator was further performed via ^{1}H NMR and ESI-TOF MS methods. In the ^{1}H NMR spectrum of the oligomer, except for the typical signals of polymer main chain, signals belonging to the pyrrolidinyl-anilido ligand could be clearly identified (Figure 7), indicating that the polymer may have the pyrrolidinyl-anilido ligand as one of the end groups. This result is further confirmed by the ESI-TOF MS (see Supporting Information), where a series of peaks systematically ended with the same group of ligand $\mathbf{L}^1$ are displayed.

All the results suggest that the bidentate pyrrolidinyl-anilido ligands in these aluminum dimethyl complexes do act as initiating groups to initiate the ROP of $\varepsilon-$CL in a living manner. It is well-known that amido groups are relatively poor in initiation when exposed to the catalytic ROP of cyclic esters. Mu and coworker[36] reported that, in the absence of alcohol, dinuclear aluminum dimethyl complexes supported by aldimine-anilido ligands were inactive toward the polymerization of cyclic esters. Thibault and Fontaine[37] found that, without the addition of alcohol, the ROP of ε-CL catalyzed by

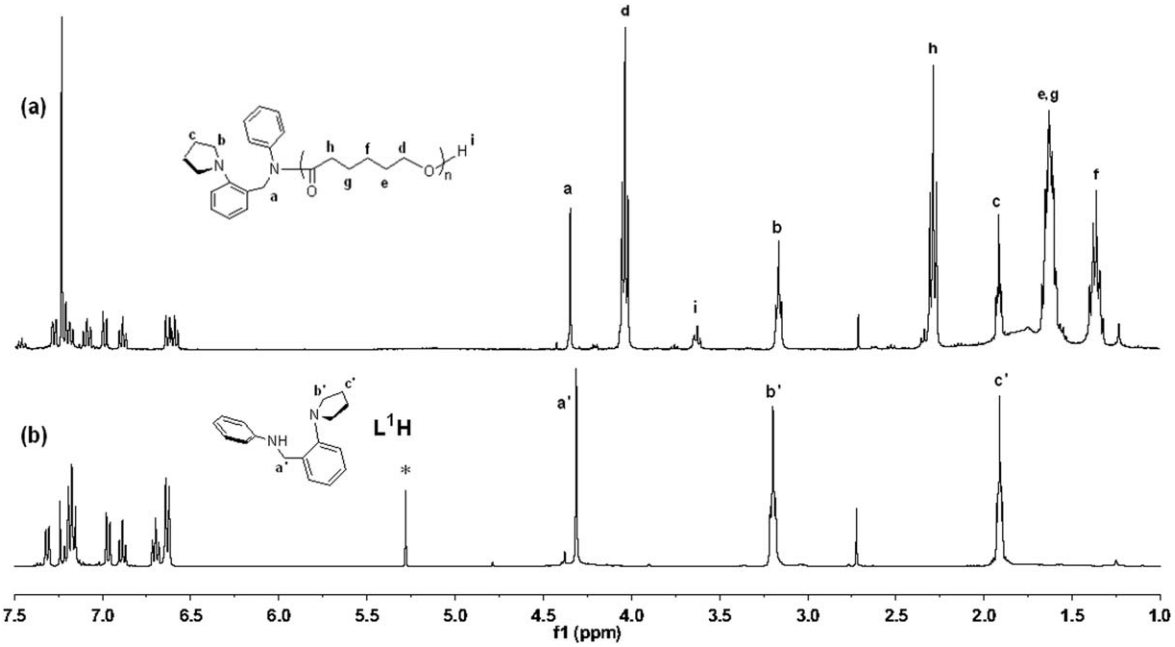

FIGURE 7 The ^{1}H NMR spectra ($CDCl_3$, 400 MHz) of (a) the oligomer of ε−CL obtained using complex **1** as initiator ([ε−CL]/[**1**] = 30, in toluene, 35 °C); (b) the proligand **L^{1}H** (*, the signal of dichloromethane).

aluminum methyl complexes with phosphine/thiol-amido ligands was badly controlled and no clear initiation mechanism could be drawn. The aluminum complexes reported in this work are rare examples that could initiate the ROP of cyclic esters with living features in addition to our previous report.[30]

Based on the above results, a coordination-insertion mechanism could be assumed for ε-CL polymerization initiated by these aluminum complexes (Scheme 2). ε−CL monomer coordinates to the aluminum center through the carbonyl oxygen to form a four-coordinated aluminum intermediate, where the pyrrolidinyl-anilido ligand is ligated monodentately. Subsequently, the amido-nitrogen atom of the ligand attacks to the carbonyl carbon of the coordinated monomer. While the acyl-oxygen bond ruptures, the oxygen atom coordinates to the aluminum metal center to produce active aluminum alkoxide species, which are in a dimeric form.[38] The ROP reaction is promoted by the continued insertion of ε−CL monomer into the active aluminum-alkoxo bonds until being quenched by wet solvent.

ROP of *rac*-LA

All aluminum complexes **1–6** were also found to be efficient initiators for the ROP of *rac*-LA. As shown in Table 2, high monomer conversions could be obtained within 15–24 h when the polymerizations were carried out in toluene at 65 °C. The resultant polymers possess narrow molecular weight distributions (M_w/M_n = 1.09–1.26), which are slightly broader than those obtained from ε−CL polymerization. Similar to the results of ε−CL polymerization, complexes **2** and **4** with an *ortho*-substituent on the anilino moiety of the ligand display relatively low catalytic activities toward the ROP of *rac*-LA, while complexes **5** and **6** with a *meta*- or *para*-chloro group are more active than the rest complexes. Therefore, the same activity order of **5** (*m*-Cl) > **6** (*p*-Cl) > **1** (H) > **3** (*p*-^{i}Pr) > **4** (*o*-Cl) > **2** (*o*-Me) is observed for complexes **1–6** toward *rac*-LA polymerization. In comparison to the previously reported piperidinyl-anilino aluminum complexes,[30] complexes **1–6** are less active, probably due to the stronger nucleophilicity of nitrogen atom of pyrrolidinyl ring. The most active complex **5** could convert 500 equiv. of *rac*-LA to high conversion of 97% within 42 h at low initiator concentration ([**5**]$_0$ = 0.005 mol/L, 85 °C in toluene). However, due to the sharply increased viscosity of the reaction mixture, the transesterification reactions became significant which led to slight broadening of the molecular distribution (M_n = 6.31 × 10^4 g/mol, M_w/M_n = 1.47). Moreover, polylactides obtained by complexes **1–6** possess atactic

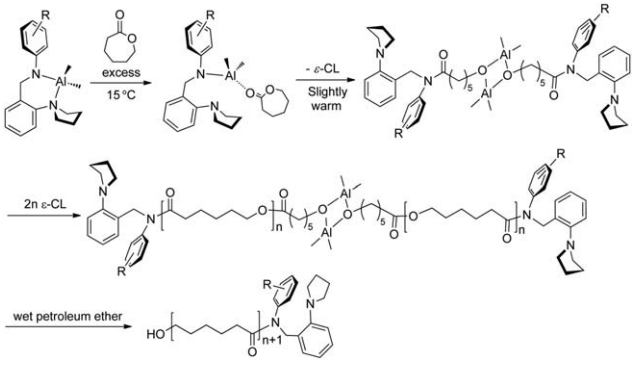

SCHEME 2 Proposed polymerization mechanism of ε−CL initiated by aluminum amido complexes.

TABLE 2 The ROP of *rac*-LA Initiated by Complexes **1–6**[a]

Run	Cat.	Time (h)	Conv. (%)[b]	$M_{n,\ calcd.}$[c] ($\times 10^4$)	$M_{n,\ NMR}$[d] ($\times 10^4$)	$M_n{}'$[e] ($\times 10^4$)	M_w/M_n[e]	P_m[f]
1	**1** (H)	15	82	1.18	1.30	1.27	1.11	0.51
2	**2** (*o*-Me)	24	88	1.27	1.29	1.18	1.15	
3	**3** (*p*-^{i}Pr)	15	78	1.12	1.20	1.09	1.09	0.50
4	**4** (*o*-Cl)	24	92	1.32	1.27	1.56	1.10	0.51
5	**5** (*m*-Cl)	15	88	1.27	1.21	1.23	1.26	
6	**6** (*p*-Cl)	15	84	1.21	1.30	1.14	1.10	0.50

[a] $[rac\text{-LA}]_0 = 1.0$ M, $[rac\text{-LA}]_0/[Al]_0 = 100$, in toluene, 65 °C.
[b] Determined by the integration ratio of the methine protons in monomer and polymer in $CDCl_3$.
[c] $M_{n,calcd.} = ([rac\text{-LA}]_0/[Al]_0) \times 144.14 \times$ conv. (%)+ mass of the free ligand.
[d] Determined by the integration ratio of the methylene protons in polymer main chain versus the characteristic resonance of the amido ligand.
[e] The number average molecular weight (M_n) and molecular weight distribution (M_w/M_n) were determined by a gel permeation chromatograph in THF at 40 °C, using narrowly distributed polystyrenes as standards, $M_n{}' = 0.58\ M_n$.
[f] P_m is the probability of forming a new *m*-dyad, determined by homonuclear decoupled ^{1}H NMR spectroscopy.

microstructures, as indicated by homonuclear decoupled ^{1}H NMR spectroscopic analyses.

For a comparison purpose, the NMR scale reactions of complex **6** with 3 equiv. of *rac*-LA in C_6D_6 at different temperatures were also monitored (see Supporting Information). As displayed in the ^{1}H NMR spectrum measured at 5 °C, the resonances belonging to complex **6** were nearly unchanged except that the two multiplets of NCH_2 (pyrrolidinyl) at 2.84 and 2.72 ppm were somewhat coalescent. This implies that the pyrrolidinyl arm might show some hemilabile coordination effect in the presence of LA monomer. After standing at 15 °C for 30 min, the signals of NCH_2 (pyrrolidinyl) became broader, and some small signals represented by peaks at 5.09, 4.78, 4.64–4.57 ppm appeared. When the mixture was kept at 15 °C overnight, the signals attributable to complex **6** almost disappeared and the above mentioned signals became dominant. The two closely located doublets at 5.09 ppm could be assigned to ArCH_2 protons of the ligand, which were in a stoichiometric ratio with the four quartets at 4.78, 4.64, 4.61, and 4.57 ppm (4:1:1:1:1) assignable to the methine protons of the inserted lactide monomers [Figure 8(a)]. Three singlets at −0.16, −0.25, and −0.40 ppm (3:6:3) accounting for Al—CH_3 protons could also be observed. Meanwhile, the signals of NCH_2 (pyrrolidinyl) obviously up-field shifted to 2.70 and 2.55 ppm (see Supporting Information), implying the dissociation of the neutral nitrogen donor from the metal center. All these features indicated the insertion of lactide monomer into Al—N (amido) bond. Two diastereomeric, lactide-inserted aluminum species in dimeric form were generated, as reported previously by Lewinski's group.[38] To further verify the dimeric nature of the monomer-inserted aluminum species, the NMR reaction of complex **6** with 2 equiv. of *L*-LA under the same

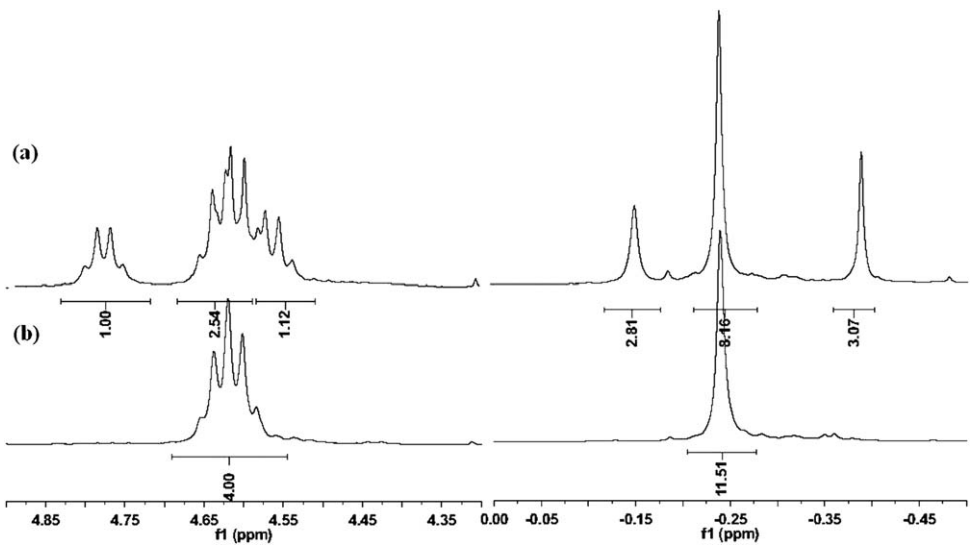

FIGURE 8 Part of ^{1}H NMR spectra (C_6D_6, 400 MHz) of (a) the reaction mixture of complex **6** and *rac*-LA ($[\mathbf{6}]_0/[rac\text{-LA}]_0 = 1{:}\ 3$) at 15 °C; (b) the reaction mixture of complex **6** and *L*-LA ($[\mathbf{6}]_0/[L\text{-LA}]_0 = 1{:}2$) at 15 °C.

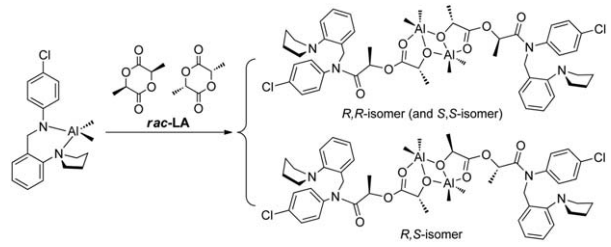

SCHEME 3 The reaction of complex **6** with *rac*-LA at ambient temperature (the structure of *S,S*-isomer is not shown).

conditions was monitored. As expected, only two closely located quartets at 4.64, 4.61 ppm and one singlet at −0.25 ppm were observed in the related regions [Figure 8(b)]. It is clear that these signals belong to the racemic *R,R*-/*S,S*-isomers and the disappeared signals belong to the *R,S*-isomer as shown in Scheme 3. The two diastereomers obtained from the reaction of complex **6** with *rac*-LA was roughly in a 2:3 molar ratio (*R,S*- isomer vs. *R,R*-/*S,S*-isomers), implying the preferable production of the *R,R*/*S,S*-isomers.

When up to about 6 equiv. of *L*-LA was added, except for the downfield shift of methine resonance of lactide monomer from 3.78 to 3.95 ppm, the other signals almost remained the same (see Supporting Information), indicating no further insertion of lactide monomer into the newly formed Al—O (lactate) bonds of the dimeric aluminum species. The polymerization was completed when warmed at 75 °C overnight. The signals accounting for the PLA main chain could be observed at 5.0 and 1.3 ppm in the ^{1}H NMR spectrum. The resonances assignable to the pyrrolidinyl-anilino ligand as well as Al—CH_3 groups although varied somewhat but still could be identified unambiguously, demonstrating the basically constant nature of the active centers during the polymerization.

According to the literature reports,[22,27,39,40] it is widely accepted that in comparison with ε−CL, lactide is in general less active toward the catalytic ROP, that is, longer reaction time or higher polymerization temperature is required for equal amount of lactide to be polymerized. It is also the case in this work. From above NMR studies, it was however found that at a relatively low temperature the insertion of lactide into the Al—N (amido) bond already occurred, while under the same conditions ε−CL monomer only coordinated to the metal center without apparent ring-opening reaction. Based on the structural characterization of a lactide-inserted, dimeric aluminum species reported by Lewinski's group,[38] it is therefore suggested that, although the insertion of the first lactide monomer might be easier than that of ε−CL monomer, the bis-chelating mode of the lactyl unit adjacent to aluminum center in the case of lactide insertion may stabilize the active center to a certain degree, which raises the energy barrier of further insertion step considerably. These results may also explain well why a random copolymerization of ε−CL and lactide could not be realized by most of the metallic initiators.

CONCLUSIONS

In conclusion, a series of aluminum dimethyl complexes bearing bidentate pyrrolidinyl-anilino ligands have been prepared and fully characterized. In the absence of a coinitiator, all the reported complexes were found to catalyze the ROPs of ε−CL and *rac*-LA in a well-controlled manner, producing polyesters with quite narrow molecular weight distributions (in most cases, $M_w/M_n = 1.04–1.15$). The catalytic activities of these aluminum complexes were affected greatly by the steric effect of the *ortho*- substituent of the anilido moiety in the ligand. The polymerization of ε−CL showed a first-order dependence on the concentrations of monomer and initiator. Polymers end-capped by the whole fragment of the pyrrolidinyl-anilino ligand were produced, which gave strong supports that the polymerization was initiated by a monomer insertion into the Al—N (amido) bond via a coordination–insertion mechanism. Based on the ^{1}H NMR scale oligomerizations, it is suggested that the insertion of the first lactide monomer might be easier than that of ε−CL monomer. The formation of dimeric aluminum species in the former case where the last lactyl unit is bis-chelating to aluminum center through alkoxy and carbonyl oxygen atoms should be responsible for the lower reactivity of lactide toward the catalytic polymerization.

ACKNOWLEDGMENTS

Financial supports from the National Natural Science Foundation of China (NNSFC, 21074032 and 21274041) and the Fundamental Research Funds for the Central Universities (WK1214048 and WD1113011) are gratefully acknowledged.

REFERENCES AND NOTES

1 S. Dagorne, D. A. Atwood, *Chem. Rev.* **2008**, *108*, 4037–4071.

2 N. E. Kamber, W. Jeong, R. M. Waymouth, R. C. Pratt, B. G. G. Lohmeijer, J. L. Hedrick, *Chem. Rev.* **2007**, *107*, 5813–5840.

3 M. O. Tina, G. W. Coates, *J. Am. Chem. Soc.* **1999**, *121*, 4072–4073.

4 T. M. Ovitt, G. W. Coates, *J. Polym. Sci. Part A: Polym. Chem.* **2000**, *38*, 4686–4692.

5 T. M. Ovitt, G. W. Coates, *J. Am. Chem. Soc.* **2002**, *124*, 1316–1326.

6 M. H. Chisholm, J. C. Gallucci, K. T. Quisenberry, Z. Zhou, *Inorg. Chem.* **2008**, *47*, 2613–2624.

7 M. H. Chisholm, N. J. Patmore, Z. P. Zhou, *Chem. Commun.* **2005**, 127–129.

8 D. Chakraborty, E. Y.-X. Chen, *Organometallics* **2002**, *21*, 1438–1442.

9 N. Nomura, A. Akita, R. Ishii, M. Mizuno, *J. Am. Chem. Soc.* **2010**, *132*, 1750–1751.

10 C. T. Chen, H. J. Weng, M. T. Chen, C. A. Huang, K. F. Peng, *Eur. J. Inorg. Chem.* **2009**, *14*, 2129–2135.

11 A. Gao, Y. Mu, J. Zhang, W. Yao, *Eur. J. Inorg. Chem.* **2009**, *24*, 3613–3621.

12 M. Shen, W. Zhang, K. Nomura, W. H. Sun, *Dalton Trans.* **2009**, *41*, 9000–9009.

13 S. Gong, H. Ma, *Dalton Trans.* **2008**, *25*, 3345–3357.

14 A. Otero, A. Lara, J. Fernandez, C. Alonso, J. A. Castro, I. Marquez, L. F. Sanchez, A. M. Rodriguez, J. C. Garcia, *Organometallics* **2011**, *30*, 1507–1522.

15 E. Kober, Z. Janas, T. Nerkowski, L. B. Jerzykiewicz, *Dalton Trans.* **2013**, *42*, 10847–10854.

16 C. Li, D. Liu, B. Ko, *Dalton Trans.* **2013**, *42*, 11488–11496.

17 S. L. Hancock, M. F. Mahon, M. D. Jones, *Dalton Trans.* **2013**, *42*, 9279–9285.

18 H. Han, Y. Liu, J. Liu, K. Nomura, Y. Li, *Dalton Trans.* **2013**, *42*, 12346–12353.

19 D. Li, Y. Peng, C. Geng, K. Liu, D. Kong, *Dalton Trans.* **2013**, *42*, 11295–11303.

20 M. H. Chisholm, C. Lin, J. C. Gallucci, B. Ko, *Dalton Trans.* **2003**, 406–412.

21 S. Qiao, W.-A. Ma, Z.-X. Wang, *J. Organometal. Chem.* **2011**, *696*, 2746–2753.

22 D. Li, Y. Peng, C. Geng, K. Liu, D. Kong, *Dalton Trans.* **2013**, *42*, 11295–11303.

23 F. Hild, L. Brelot, S. Dagorne, *Organometallics* **2011**, *30*, 5457–5462.

24 C. Bakewell, R. H. Platel, S. K. Cary, S. M. Hubbard, J. M. Roaf, A. C. Levine, A. J. P. White, N. J. Long, M. Haaf, C. K. Williams, *Organometallics* **2012**, *31*, 4729–4736.

25 F. Hild, L. Brelot, S. Dagorne, *Organometallics* **2011**, *30*, 5457–5462.

26 X.-F. Yua, Z.-X. Wang, *Dalton Trans.* **2013**, *42*, 3860–3868.

27 D. Ilaria, L. Marina, M. Mina, M. Stefano, P. Claudio, *J. Polym. Sci. Part A: Polym. Chem.* **2014**, *52*, 49–60.

28 F. Qian, K. Liu, H. Ma, *Dalton Trans.* **2010**, *39*, 8071–8083.

29 F. Qian, K. Liu, H. Ma, *Chin. J. Catal.* **2011**, *32*, 189–1195.

30 J. Liu., H. Ma, *Dalton Trans.* **2014**, *43*, 9098–9110.

31 R. L. Bentley, H. Suschitzky, *J. Chem. Soc. Perkin Trans. 1* **1976**, *16*, 1725–1734.

32 G. M. Sheldrick, *Acta Crystallogr. Sect. A* **2008**, *64*, 112−122.

33 SADABS, Bruker Nonius Area Detector Scaling and Absorption Correction-V2.05, Bruker AXS Inc.: Madison, WI, **1996**.

34 C. K. Johnson, ORTEP-III: A FORTRAN Thermal Ellipsoid Plot Program for Crystal Structure Illustrations, Report ORNL5138, Oak Ridge National Laboratory, Oak Ridge, TN, USA, **1976**.

35 I. Barakat, P. Dubois, R. Jerome, P. Teyssie, *J. Polym. Sci. A: Polym. Chem.* **1993**, *31*, 505–514.

36 W. Yao, Y. Mu, A. Gao, W. Gao, L. Ye, *Dalton Trans.* **2008**, 3199–3206.

37 M. H. Thibault, F. G. Fontaine, *Dalton Trans.* **2010**, *39*, 5688–5697.

38 J. Lewinski, P. Horeglad, K. Wojcik, I. Justyniak, *Organometallics* **2005**, *24*, 4588–4593.

39 S. Dagorne, F. L. Bideau, R. Welter, S. Bellemin-Laponnaz, A. Maisse-François, *Chem. Eur. J.* **2007**, *13*, 3202–3217.

40 F. Hild, N. Neehaul, F. Bier, M. Wirsum, C. Gourlaouen, S. Dagorne, *Organometallics* **2013**, *32*, 587–598.